Optimizing Runway Orientation: A Fine-Scanning Algorithm and Continuous Area Integration Approach

Trong Hiep Nguyen
Faculty of Civil Engineering, University of Transport and Communications, Hanoi, Vietnam
nguyentronghiep@utc.edu.vn (corresponding author)

Huy Khang Pham
Faculty of Civil Engineering, University of Transport and Communications, Hanoi, Vietnam
phkhangdr@utc.edu.vn

Received: 22 January 2026 | Revised: 28 February 2026 and 15 March 2026 | Accepted: 24 March 2026

 DOI: https://doi.org/10.48084/etasr.17706

ABSTRACT

Optimal runway orientation is a determinant of airport operational safety and capacity, governed by the requirement to maximize the Usability Factor (UF) under adverse crosswind conditions. Traditional planning methodologies, specifically the graphical wind rose technique and some computational models, often rely on coarse 10-degree increments or linear approximations. This approach may induce a "precision gap" that fails to capture the true mathematical optimum when processing grouped meteorological data. This study introduces V-ROpt, a high-precision automated framework that utilizes Continuous Area Integration (CAI) logic to resolve the partial coverage problem within 16-direction wind sectors. By implementing an exhaustive fine-scanning algorithm at 0.5-degree resolution, the framework minimizes discretization error inherent in conventional techniques. The numerical results demonstrate that V-ROpt can identify a localized optimum representing a 1.0-degree shift from traditional 10-degree methods, achieving a marginal usability improvement of 0.03%. For complex airfield configurations, where a single runway fails to meet the required 95% UF, the proposed framework generates a portfolio of the top 5 optimal crosswind runway scenarios. The computational results demonstrate that the proposed crosswind runway orientations improved the combined UF by 6.38%-7.76% compared to the single-runway configuration, which initially provided a UF of only 91.08%. This enables planners to perform trade-off analyses between aerodynamic efficiency and physical constraints, such as terrain, obstacle limitation surfaces, or other environmental constraints.

Keywords-runway orientation; wind coverage; usability factor; continuous area integration; grouped wind data; crosswind runway; fine-scanning

I. INTRODUCTION

During takeoff and landing operations, aircraft are significantly impacted by crosswind conditions. When high-velocity crosswinds occur at an airport, pilots must execute crab angle adjustments or heading corrections during the final approach (Figure 1). This procedure represents a complex technical challenge that directly compromises operational flight safety. Therefore, the determination of runway orientation is a crucial task in airport master planning, as the alignment of the primary runway dictates the configuration of terminal facilities, taxiway networks, and the overall operational safety of the airfield [1, 2].

To maintain the highest safety margins during takeoff and landing, international regulatory bodies have established rigorous standards based on the prevailing wind distribution. Specifically, the International Civil Aviation Organization (ICAO), Federal Aviation Administration (FAA), and Civil Aviation Authority of Vietnam (CAAV) stipulate that runways must be oriented to ensure a Usability Factor (UF) of at least 95% [3, 4]. This metric requires that the Crosswind Component (CWC) does not exceed the Allowable Crosswind Component (*ACC*), ranging from 10.5 to 20 knots, determined by the aircraft's Runway Design Code (RDC), which considers approach speeds and wingspans. According to ICAO and CAAV regulations, the *ACC* values are 10, 13, and 20 knots, approximately corresponding to 19, 13, and 37 km/h contingent upon the aerodrome reference field length of the aircraft, which is defined as the minimum takeoff distance required by an aircraft under standard conditions, including the mean sea level, standard atmospheric pressure, zero wind, and zero runway gradient. Table I illustrates the specific allowable crosswind velocity thresholds prescribed by these international and domestic standards [4, 5].

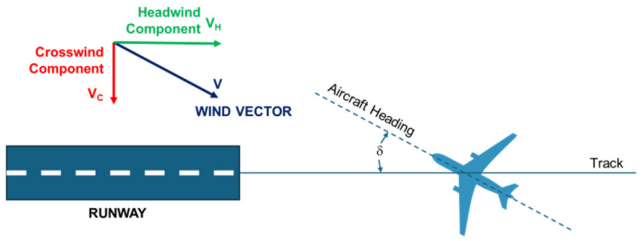

Fig. 1. Principle of runway orientation under crosswind conditions.

TABLE I. REGULATIONS OF ALLOWABLE CROSSWIND VELOCITY OF RUNWAY

Criteria	FAA (AC 150/5300-13B)[a]	ICAO (Annex 14, Vol 1)[b]
10 / 10.5 knots limit	10.5 knots A-I and B-I (including small aircraft)	10 knots (19 km/h) RL< 1,200 m
13 knots limit	13 knots A-II and B-II	13 knots (24 km/h) 1,200 m ≤ RL < 1,500 m
16 knots limit	16 knots A-III, B-III, C-I through D-III	(not specified)
20 knots limit	20 knots A-IV and B-IV, C-IV through C-VI, D-IV through D-VI, E-I through E-VI	20 knots (37 km/h)[c] RL ≥ 1,500 m or over

[a] Based on RDC, comprising aircraft approach category and Airplane Design Group (ADG).

[b] Based on Aeroplane Reference Field Length (RL)

[c] Limit reduced to 13 knots when runway braking action is poor

The economic implications of runway orientation are profound. Modern greenfield airport projects or major global hubs involve capital expenditure ranging from several hundred million to billions of dollars. A sub-optimal primary runway orientation not only compromises safety but may also trigger the premature need for a crosswind runway, increasing land acquisition costs and environmental footprints. Furthermore, daily operational efficiency is tied to wind alignment; poor orientation leads to increased diversions, higher fuel consumption during the approach, and reduced airfield capacity. This can also indirectly influence the strategic prioritization of upgrading the infrastructure systems of existing airfields in the future [2, 5].

Despite its importance, the methodology for determining the orientation has remained largely stagnant. The traditional "wind rose" method, while intuitive, is prone to human error and visual estimation bias. Modern computational tools often simplify the problem by using 10-degree sectors, which correspond to the standard grouping of meteorological data. However, wind is a continuous physical phenomenon. Treating it as discrete blocks leads to information loss, particularly when the runway's allowable crosswind "template" intersects only a portion of a wind sector, a challenge known as the partial coverage problem [6-9].

Historically, this orientation was determined using the wind rose method, a graphical vector analysis where a transparent template representing the *ACC* is rotated over a polar plot of wind data. While crucial, this manual technique relies on visual estimation and assumes a uniform distribution of wind within sectors, which can lead to inaccuracies in maximizing capacity [1, 4, 5, 10].

The transition from manual graphical methods to computational models is marked by three significant contributions. First, authors in [9] established a statistical foundation by applying a bivariate normal elliptical distribution to wind components, allowing for the minimization of theoretical crosswind probabilities without relying solely on empirical plots. After that, authors in [6] advanced the field by digitalizing the FAA standards using the VB-WNDROS model. This object-oriented automation converted graphical sectors into Cartesian coordinates, effectively solving the partial coverage problem and eliminating manual plotting errors. Subsequently, authors in [8] introduced the Calculation of Optimum Runway Orientation (CORO) model. Unlike predecessors that used grouped wind data, CORO processed individual wind observations directly, thereby bypassing the FAA's assumption of uniform wind distribution within sectors to enhance mathematical precision.

Applied research has broadened the scope of optimization tools. Authors in [7] integrated the wind rose method with Geographic Information Systems (GIS) spatial analysis, enabling the visualization of runway orientation within geospatial databases. Regional-specific tools were developed in [11] for Iraq and in [2] for Egypt, validating automated results against manual methods for local airport master planning. Authors in [12] highlighted that ignoring wind gusts can compromise safety and proposed a gust factor to conservatively estimate the peak crosswinds. Furthermore, authors in [13] utilized C-programming to develop search algorithms that rapidly calculate geometric standards and corrections alongside orientation.

The OMRO model developed in [14] is an analytical spreadsheet-VBA tool that optimizes runway orientations through precise wind coverage analysis. Moving beyond the visual estimation of traditional wind rose methods, this model uses trigonometric "what-if" equations to calculate an adjustment factor (*f*) for partially covered wind sectors.

Meteorological stations typically report wind data in 16 or 36 directions. When these data are grouped into sectors, it is often assumed that the wind frequency is uniformly distributed within that arc. When a runway template (representing the *ACC*) is overlaid, it may cut through the sector at an arbitrary angle. Traditional models either include the entire sector's frequency or exclude it based on the sector's centerline.

V-ROpt resolves this by calculating the exact geometric intersection area, ensuring that every fraction of a percentage of wind frequency is accounted for. The input wind data format is 16-direction (22.5 degrees for each sector), which complies with local standards in determining runway orientation for airport design missions [15-17].

II. METHODOLOGY

A. Optimization of Wind Coverage $W(\theta)$ as a Continuous Function

The primary objective is to maximize the UF or wind coverage $W(\theta)$, which represents the probability that the CWC does not exceed the ACC for a given runway orientation θ. The V-ROpt framework defines $W(\theta)$ as a continuous function of the azimuth $\theta \in [0, 180°)$.

The objective function derived from the grouped data can be expressed as the integration of wind probabilities over the safe operational area $S(\theta)$, as shown in:

$$W(\theta) = \iint_{S(\theta)} f(v, \phi)\, dv\, d\phi \approx$$

$$\approx P_{calm} + \sum_{i=1}^{N} \sum_{j=1}^{M} P_{i,j} \cdot \alpha_{i,j}(\theta, ACC) \quad (1)$$

where $f(v, \phi)$ is the joint probability density function of wind speed v and direction ϕ, P_{calm} is the relative frequency of calm wind conditions, $S(\theta)$ is the region within the wind rose defined by the runway safety template at orientation θ, $P_{i,j}$ is the relative frequency of wind in speed group i and direction sector j from the grouped data, and $\alpha_{i,j}(\theta, ACC)$ is the partial coverage ratio for orientation θ and threshold ACC.

B. Continuous Area Integration Logic and Partial Coverage Formula

The partial coverage problem is defined as the area that the rectangular runway safety template intersects only a fraction of a polar wind sector. The Continuous Area Integration (CAI) employed in the V-ROpt framework calculates the specific intersection ratio $\alpha_{i,j}(\theta, ACC)$:

$$\alpha_{i,j}(\theta, ACC) = \frac{\text{Area}\left(\text{Sector}_{i,j} \cap \text{Template}(\theta, ACC)\right)}{\text{Area}\left(\text{Sector}_{i,j}\right)} \quad (2)$$

where $\text{Sector}_{i,j}$ denotes the polar area defined by the wind speed boundaries $[v_{i,min}, v_{i,max}]$ and direction limits $[\phi_{j,start}, \phi_{j,end}]$, and Template (θ, ACC) represents the geometric area where the CWC is within the allowable limit ACC for the orientation θ.

This converts the graphical "wind rose" method into a precise coordinate-based numerical integration.

C. Crosswind Formulation and Fine-Scanning Resolution

The main constraint governing the safety template is the CWC. For any wind vector with speed V and direction ϕ, relative to a runway orientation θ, the CWC V_c is derived as:

$$V_c = V \cdot \sin |\, (\phi - \theta)\, | \leq ACC \quad (3)$$

Assuming a uniform wind distribution within each sector, the representative velocity is defined as the average of v_{min} and v_{max}, while the wind frequency is considered to be evenly distributed throughout the sector's angular and radial span.

To ensure precision, V-ROpt implements a fine-scanning algorithm with a resolution of $\Delta\theta = 0.5°$. This high-resolution scan minimizes the discretization error inherent in grouped data analysis, ensuring that the identified θ_{opt} is closer to the true mathematical global maximum.

D. Dual-Phase Search Logic

The optimization proceeds via a dual-phase search algorithm to address multi-runway configurations based on the following logic:

Phase 1 (primary runway R_1): An exhaustive search is performed over $\theta \in [0, 180°)$ to find θ_{opt1} maximizing $W(\theta)$:

$$\theta_{R1} = \arg\max_{\theta} W(\theta) \quad (4)$$

Phase 2 (crosswind runway R_2 portfolio): If $W(\theta_{R1}) < 95$, the algorithm fixes R_1 and initiates a secondary search for R_2. It evaluates the combined coverage using the inclusion-exclusion principle:

$$W_{combined} = W(R_1) + W(R_2) - W(R_1 \cap R_2) \quad (5)$$

Instead of a single output, V-ROpt generates a portfolio of the Top 5 optimal R_2 scenarios for consideration in airport planning.

III. ALGORITHM DEVELOPMENT

A. Dual-Phase Search Framework

The computational structure of V-ROpt was developed as a dual-phase search framework, as illustrated in Figure 2.

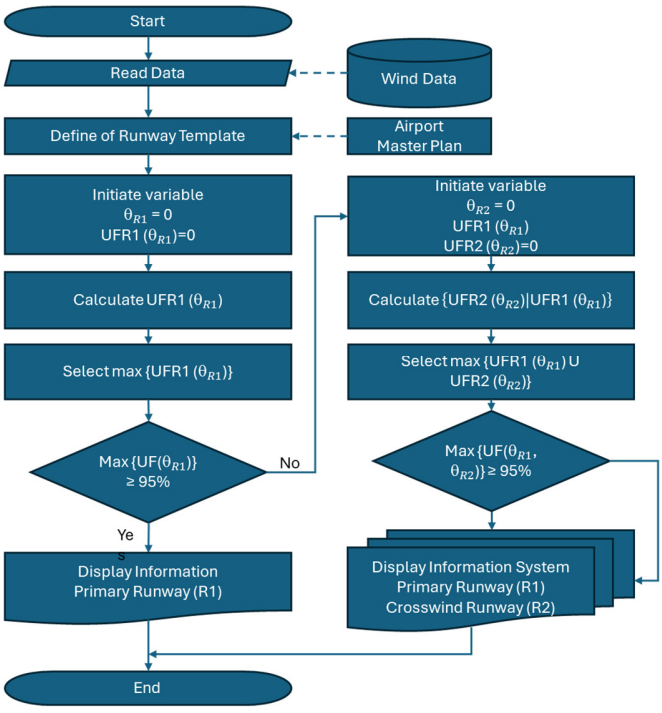

Fig. 2. Algorithm of runway orientation V-ROpt program.

The V-ROpt framework executes a dual-phase search heuristic designed to identify the absolute global maximum for wind coverage across single and multiple runway configurations. In the primary phase, the algorithm ingests standardized meteorological wind data and initializes the

runway orientation variable θ. The core engine performs an exhaustive 360-iteration loop to compute the UF for the primary runway (R_1).

If the maximum identified UF(R_1) meets or exceeds the mandatory 95% safety threshold defined by ICAO and FAA standards, the system terminates the search and displays the optimal orientation. Nevertheless, if R_1 fails to provide sufficient coverage, the algorithm triggers phase 2, fixing the optimal R_1 and initializing a secondary search for a crosswind runway (R_2). This phase evaluates the combined systemic coverage through the inclusion-exclusion principle to maximize incremental wind capture. To facilitate robust decision-making under physical terrain constraints, the framework concludes by generating a strategic portfolio of the top five optimal multi-runway scenarios, rather than a single discrete solution. The detailed logic of the V-ROpt is presented in the pseudo code below:

```
Algorithm: V-ROpt Dual-Phase Optimization
Input: Grouped wind dataset P_{i,j} (velocity i, direction j); Allowable Crosswind Component ACC.
Output: Optimal primary azimuth θ_{R1}; Top-5 crosswind runway configurations R_2.
1: Initialization of scanning resolution Δθ = 0.5° and range θ ∈ [0, 180°].
2: Phase 1: Primary Runway (R1) Search
3: For each θ_k from 0 to 180 step Δθ do
4:  Construct runway safety template at orientation θ_k
5:  For each wind in (i,j) in P_{i,j} do
6:   Calculate α_{i,j}(θ_k) using (2)
7:   Update UF(θ_k) using (1).
8:   End For
9:  End For
10: Identify θ_{R1} = argmax UF(θ_k).
11: If UF(θ_{R1}) ≥ 95 then
12:   Return θ_{R1} and Terminate
13: Else
14:   Phase 2: Crosswind Runway (R2) Search
15:   Fix primary orientation at θ_{R1}.
16:   For each θ_m from 0 to 180 step Δθ do:
17:    Compute combined system coverage W_{combined} using (5)
18:   End For
19:   Sort all θ_m results by W_{combined} in descending order
20:   Return Top-5 optimal scenarios for R_2 portfolio.
21: End If
```

The computational complexity of the V-ROpt framework is defined by the exhaustive search across the orientation domain. For the primary runway (R_1) optimization, the complexity is $O(k \cdot n \cdot m)$, where k represents the number of scanning steps ($k = 180/\Delta\theta$), n is the number of wind velocity groups, and m is the number of directional sectors. At a fine-scanning resolution of $\Delta\theta = 0.5°$, the algorithm performs 360 iterations.

Despite the increased resolution compared to traditional 10-degree methods, the CAI logic remains computationally efficient. Phase 2 for crosswind runway (R_2) portfolio generation maintains a similar complexity, with an additional overhead for inclusion-exclusion area calculations.

B. V-ROpt Input/Output and Performance

The input for V-ROpt consists of a wind frequency dataset categorized into 16 directions and recorded velocity levels. Additionally, users must specify the allowable crosswind velocity limits for the airport's runway system. Upon execution, V-ROpt generates comprehensive reports, including wind rose diagrams and stacked bar charts for input data visualization. The framework identifies the optimal orientation and the UF for the primary runway. In cases where the primary runway's UF falls below the 95% threshold, the program determines the optimal configuration for a crosswind runway, providing both the individual UF for the secondary runway and the combined UF for the entire system. The typical processing time for V-ROpt is within a few minutes, and the results can be exported as a summary report.

IV. EXAMPLES AND DISCUSSION

A. Examples

To evaluate the operational performance of V-ROpt, the sample data from Table 6-4 of [10] were utilized as the computational input for all three examples presented in this section. This dataset comprises wind frequencies across 16 directions and 5 velocity categories, originally recorded in miles per hour (mi/h). For consistency with standard aviation practices, all wind velocities within the framework were converted to knots (1 knot = 1.151 mi/h = 1.852 km/h). The original wind frequency distribution was reconstructed and visualized through the wind rose and cumulative frequency diagrams illustrated in Figure 3.

The assessment is divided into three distinct computational examples. Example 1 conducts a sensitivity analysis of the primary runway UF based on scanning resolutions of 10°, 5°, and 0.5° configured within V-ROpt. The *ACC* used for this calculation was $V_{ACC} = 20$ knots. Example 2 evaluates the primary runway for the remaining four FAA-regulated crosswind velocity thresholds: 16, 13, and 10.5 knots. The scanning resolution was fixed at 0.5°. Example 3 focuses on identifying the Top 5 strategic orientations for a crosswind runway (R_2) in which the primary runway fails to meet the minimum UF requirement (UF < 95%) identified in Example 2. The objectives and calculations in the examples are summarized in Table II.

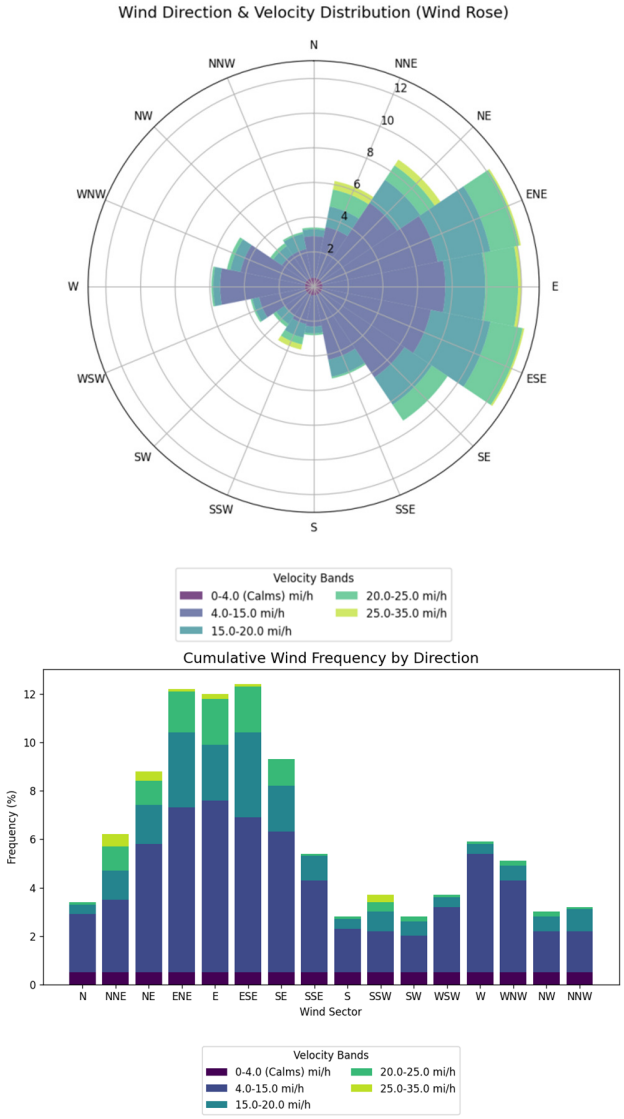

Fig. 3. Wind data demonstrated as a wind rose and cumulative diagrams.

TABLE II. EXAMPLES

Examples	Objective	Scanning step (Degree)	*ACC* (knots)
Example 1	Sensitive analysis scanning step	10, 5, 0.5	20
Example 2	Primary runway orientation	0.5	16, 13, 10.5
Example 3	Crosswind runway proposal	0.5	01 scenario of crosswind runway required

1) Example 1: Sensitivity Analysis by Scanning Resolution

This example examines two factors: the variation in UF and the corresponding runway azimuth direction. Table III presents the UF values and runway headings calculated by V-ROpt at scanning steps $\Delta\theta$ of 10°, 5°, and 0.5°. The experimental results demonstrated that the scanning step influenced both the optimal direction and calculated usability. Specifically, standard 10° and 5° steps, corresponding to Figures 4 and 5, respectively, failed to capture the localized extrema of the usability function. The 0.5° fine-scanning resolution (Figure 6) reveals the UF peaks with higher precision. While the numerical change in the UF might appear marginal (-0.03%), the optimal runway azimuth shifts by 1.0° when moving from coarse to fine scanning. Figure 7 depicts the optimum location of the runway on wind rose diagram, at azimuth of 61.0° and UF of 99.94%.

TABLE III. SCANNING RESULTS

Scanning step (degrees)	Azimuth of primary runway R_1 (degrees)	UF of runway R_1 (%)	Deviation from optimum (%)
10	60	99.91	-0.03
5	60	99.91	-0.03
0.5	61.0	99.94	Optimum

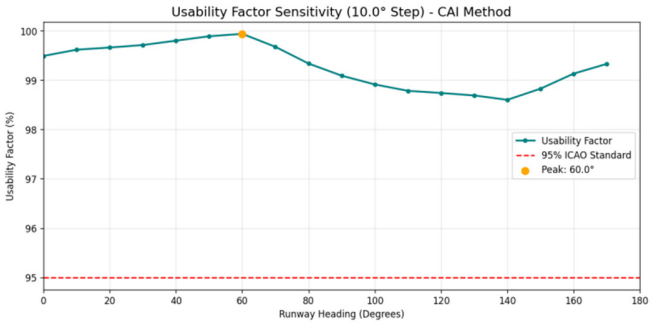

Fig. 4. UF of the primary runway corresponding 10-degree scanning step.

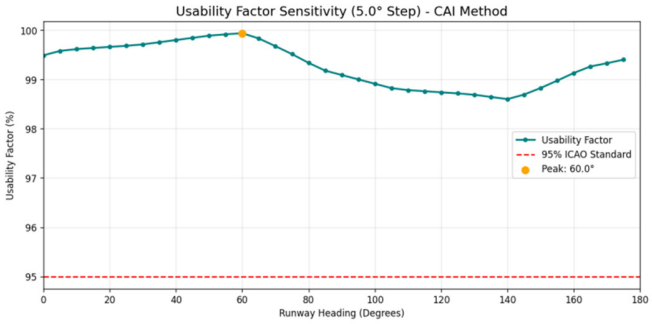

Fig. 5. UF of the primary runway corresponding 5-degree scanning step.

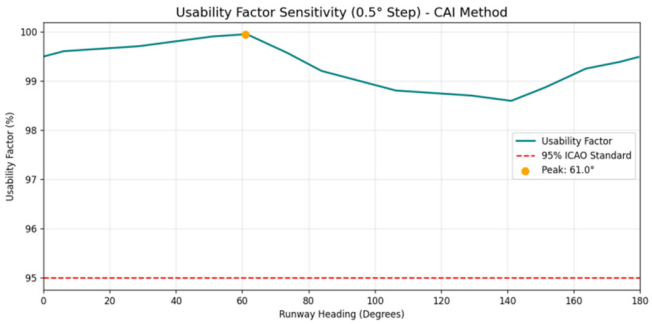

Fig. 6. UF of the primary runway corresponding 0.5-degree scanning step.

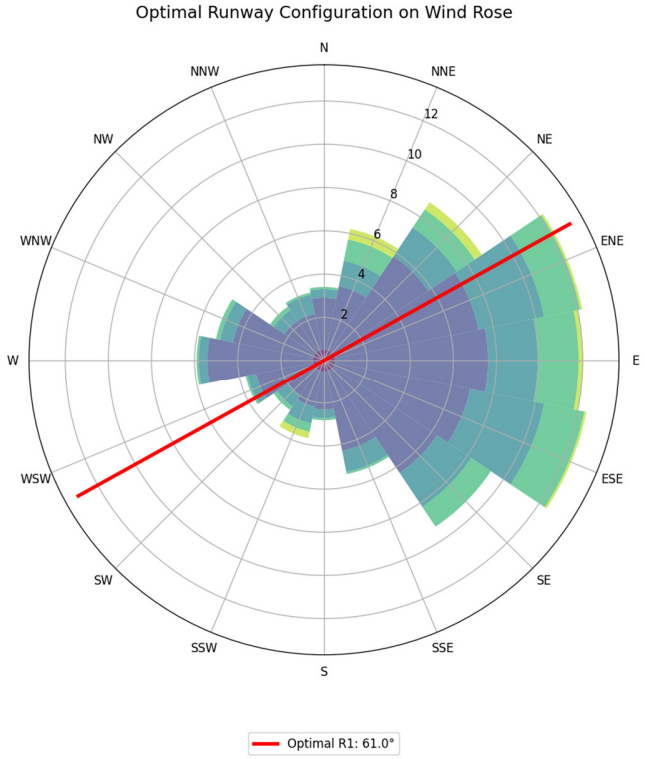

Fig. 7. The direction of the primary runway on the wind rose corresponding to a 0.5-degree step.

2) Example 2: Primary Runway (R_1) Optimization at Various Velocity Limits

In this example, V-ROpt performed to find the optimal primary runway (R_1) orientation at the 0.5° resolution for the remaining FAA crosswind limits: 16, 13, and 10.5 knots (cases 2-1, 2-2, and 2-3). As shown in Table IV, the UF values for these cases were 97.36%, 91.08%, and 86.89%, respectively. Since the last two cases (2-2 and 2-3) yielded UFs below the mandatory 95% threshold, the V-ROpt framework automatically issued a recommendation for the implementation of a crosswind runway system to enhance overall airfield usability.

TABLE IV. EXPERIMENTAL RESULTS

Example	Velocity limits of crosswind (knots)	Azimuth of primary runway R_1 (Degree)	UF of runway R_1 (%)	Crosswind runway requirement
Case 2-1	16	68.0	97.36	Not required
Case 2-2	13	88.0	91.08	Needed
Case 2-3	10.5	91.5	86.89	Needed

3) Example 3: Crosswind Runway (R_2) Portfolio Generation

Based on the results from Example 2, case 2-2 was selected to determine the optimal crosswind runway configuration tailored to the airport's specific conditions. Using the wind data from Example 2 and assuming an *ACC* of $V_{ACC} = 13$ knots, V-ROpt generated a portfolio of the top 5 optimal crosswind runway orientations. The results in Table V indicate that all five R_2 (rank 1st-rank 4th) configurations successfully elevated the combined system usability to values greater than 95%. In addition to the aggregate system usability, V-ROpt provides the incremental coverage contributed by the crosswind runway. The optimal dual-runway configuration, comprising the primary runway and the R_2 orientation with the highest contribution, is visualized on the wind rose in Figure 8.

TABLE V. TOP 5 CONFIGURATIONS FOR CROSSWIND RUNWAY – EXAMPLE 2.2

Rank	R_2 azimuth (degrees)	Runway R_2 coverage (%)	Combined coverage (%)	Extra (%)
1	25.5	82.42	98.84	+7.76
2	4.5	82.24	98.81	+7.73
3	179.5	82.08	98.67	+7.59
4	164.5	82.73	97.74	+6.66
5	40.5	86.13	97.46	+6.38

As illustrated in the charts in Figure 3, while the ENE, E, and ESE directions exhibited high cumulative wind frequencies exceeding 12%, the NNE, NE, and SSW directions showed significantly higher frequencies of high-velocity winds.

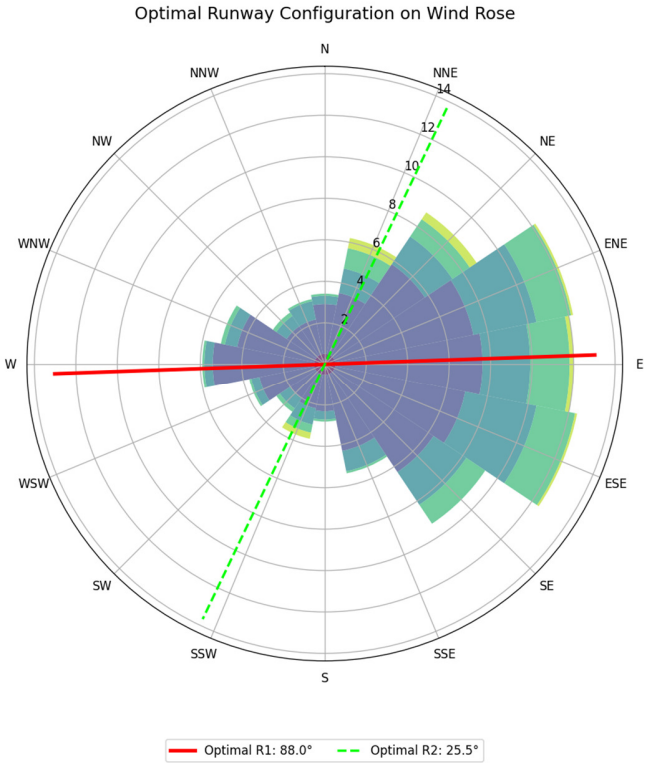

Fig. 8. The optimum azimuth of the runway configuration on the wind rose.

This heterogeneous distribution between wind frequency and velocity intensity complicates the manual determination of the optimal runway orientation. Since the NNE, NE, and SSW sectors are characterized by strong wind currents, they pose the greatest crosswind risks to East-West oriented runways. The computational results from V-ROpt accurately resolve this trade-off by identifying a specific heading that minimizes the

penetration of these high-velocity wind bands into the allowable crosswind limits.

B. Discussion

While the V-ROpt computational framework has demonstrated rapid and precise capabilities in optimizing both single primary runways and combined primary-crosswind runway systems, certain assumptions and limitations must be clarified for its practical application.

First, a significant assumption of this study is that the wind is uniformly distributed within each individual 22.5-degree meteorological sector. Although the application of the CAI logic combined with a fine-scanning step provides rapid and precise computational results, the output remains dependent on the quality and resolution of the input grouped wind data. In cases where raw, non-grouped wind observations are available, future enhanced versions of the model could integrate non-parametric density estimation methods to further refine the calculation of the UF.

Second, the current scope of the optimization framework is focused exclusively on CWC constraints as regulated by aviation authorities such as ICAO, FAA, or CAAV. In practical airport master planning, the determination of runway orientation is also influenced by various operational and environmental factors. These include headwind and tailwind requirements for takeoff and landing performance, Obstacle Limitation Surfaces (OLS), noise abatement procedures, local terrain constraints, and adjacent urban development objectives.

Finally, although the high-resolution 0.5-degree scanning yields a marginal UF improvement (~0.03%) in most scenarios, its true value lies in borderline decision-making. For airports struggling to meet the 95% minimum requirement, the 1.0-degree orientation shift identified by the framework can represent the difference between regulatory compliance and the costly necessity of an additional crosswind runway. Consequently, despite the subtle mathematical gain, the strategic implications for infrastructure investment and safety risk management are significant.

V. CONCLUSIONS

This study introduces the V-ROpt framework and its corresponding computational implementation as a primary automated solution for airport planners, enhancing decision-support in runway orientation optimization under wind constraints. By integrating the Continuous Area Integration (CAI) method, the framework significantly accelerates the processing speeds. In addition, the application of high-resolution scanning facilitates the identification of Usability Factor (UF) peaks that are potentially bypassed by coarser traditional increments. Minor adjustments in runway azimuth-down to a 0.5° resolution can refine the UF, thereby potentially improving the operational availability of the airfield.

The proposed framework also effectively identifies optimal crosswind runway orientations when the primary runway fails to meet the mandatory 95% usability threshold. This feature is particularly advantageous for airports located in areas affected by dispersed wind patterns and/or high-velocity conditions. Moreover, by providing a portfolio of the Top 5 primary-crosswind runway configurations, the V-ROpt framework enables planners to perform critical trade-off analyses between aerodynamic efficiency and site-specific constraints, such as terrain, obstacles, emissions, and noise, ensuring a more balanced and feasible infrastructure development.

Future work will focus on enhancing the program architecture, expanding input data compatibility, and developing embedded modules for integration with Geographic Information Systems (GIS) to systematically account for topographical, obstacle, or environmental constraints during airport runway orientation.

DECLARATION OF COMPETING INTERESTS

The authors declare no competing interests.

ACKNOWLEDGMENT

This research was funded by the University of Transport and Communications (UTC) under grant number T2025-CT-007.

DATA AVAILABILITY

The wind frequency data used in this study were based on real-world meteorological records from the standard dataset (Table 6-4) in [10] converted to knots for aviation consistency.

AI USE AND DECLARATION OF GENERATIVE AI USE

The authors used Gemini and ChatGPT only for language polishing and grammatical corrections. No AI was used for data generation or original scientific analysis.

REFERENCES

[1] N. J. Ashford, S. Mumayiz, and P. H. Wright, *Airport Engineering: Planning, Design, and Development of 21st Century Airports*. Hoboken, N.J: Wiley, 2011.

[2] E.-S. M. Abdalla, M. Enieb, and R. N. A. E. Mohamed, "Investigation in Selecting the Optimum Airport Runway Orientation with Special Reference to Egyptian Airports," *Journal of Engineering Sciences*, vol. 39, no. 6, pp. 1261–1280, Nov. 2011, https://doi.org/10.21608/jesaun.2011.112516.

[3] *Aerodromes: Aerodrome Design and Operations. Annex 14 to the Convention on International Civil Aviation*, 8th ed., vol. 1. Montreal, Canada: International Civil Aviation Organization, 2018.

[4] *AC 150/5300-13B - Airport Design*. Washington D.C., USA: Federal Aviation Administration, 2022.

[5] R. de Neufville and A. Odoni, *Airport Systems: Planning, Design, and Management*, 2nd ed. London: McGraw-Hill Professional, 2003.

[6] R. M. Mousa, "Enhancement of WNDROS Program for Optimization of Runway Orientation," *Designing, Constructing, Maintaining, and Financing Today's Airport Projects*, pp. 1–11, Apr. 2012, https://doi.org/10.1061/40646(2003)4.

[7] X. Jia, D. Chung, J. Huang, M. Petrilli, and L. The, "ARO: Geographic Information Systems-Based System for Optimizing Airport Runway Orientation," *Journal of Transportation Engineering*, vol. 130, no. 5, pp. 555–559, Sept. 2004, https://doi.org/10.1061/(ASCE)0733-947X(2004)130:5(555).

[8] H. Oktal and N. Yildirim, "New Model for the Optimization of Runway Orientation," *Journal of Transportation Engineering*, vol. 140, no. 3, Mar. 2014, Art. no. 04013020, https://doi.org/10.1061/(ASCE)TE.1943-5436.0000637.

[9] L. W. Falls and S. C. Brown, *Optimum runway orientation relative to crosswinds, Technical Note TN D-6930*. USA: NASA, 1972.

[10] R. M. Horonjeff, F. X. McKelvey, W. J. Sproule, and S. Young, *Planning and Design of Airports*, 5th ed. New York: McGraw Hill, 2010.

[11] S. I. Sarsam and H. A. Ateia, "Development of a Computer Program for Airport Runway Location, Orientation, and Length Design in Iraq," in *Transportation and Development Institute Congress 2011*, Mar. 2011, pp. 291–300, https://doi.org/10.1061/41167(398)29.

[12] R. Bellasio, "Analysis of wind data for airport runway design," *Journal of Airline and Airport Management*, vol. 4, no. 2, pp. 97–116, Sept. 2014, https://doi.org/10.3926/jairm.26.

[13] S. L. Chowhan, V. K. Kumar, and S. R. Kumar, "Runway Orientation and Designing," *Indian Journal of Scientific Research*, vol. 17, no. 2, pp. 136–141, 2018.

[14] S. Chang, "Crosswind-based optimization of multiple runway orientations," *Journal of Advanced Transportation*, vol. 49, pp. 1–9, Jan. 2015, https://doi.org/10.1002/atr.1247.

[15] *All-weather operations, TCCS 19:2016/CHK*. Hanoi, Vietnam: Civil Aviation Authority of Vietnam, 2016.

[16] *Aerodromes - General Requirements, TCVN 8753:2011*. Hanoi, Vietnam: Ministry of Science and Technology of Vietnam, 2011.

[17] *Aerodrome - Runway - Specification for Design, TCVN 11364:2016*. Hanoi, Vietnam: Ministry of Science and Technology of Vietnam, 2016.